ORIGINAL ARTICLE

Insights into the relationship between hydraulic safety, hydraulic efficiency and tree structural complexity from terrestrial laser scanning and fractal analysis

Yonten Dorji[1,2] · Emilie Isasa[3] · Kerstin Pierick[1] · Juliano Sarmento Cabral[4,5] · Tashi Tobgay[2] · Peter Annighöfer[6] · Bernhard Schuldt[3,7] · Dominik Seidel[1]

Abstract

Key message **This research focused on the interplay between tree structural complexity and drought tolerance, unraveling the crucial role of D_b as an indicator of hydraulic efficiency and vulnerability in several tree species.**

Abstract The potential of trees to adapt to drier and hotter climates will determine the future state of forests in the wake of a changing climate. Attributes connected to the hydraulic network are likely to determine a tree's ability to endure drought. However, how a tree's architectural attributes related to drought tolerance remains understudied. To fill this gap, we compared the structural complexity of 71 trees of 18 species obtained from terrestrial laser scanning (TLS) with key hydraulic thresholds. We used three measures of xylem safety, i.e., the water potential at 12%, 50%, and 88% loss of hydraulic conductance (P_{12}, P_{50}, P_{88}) and specific hydraulic conductivity (K_s) to assess the trees' drought tolerance. TLS data were used to generate 3D attributes of each tree and to construct quantitative structure models (QSMs) to characterize the branching patterns. Fractal analysis (box-dimension approach) was used to evaluate the overall structural complexity of the trees (D_b) by integrating horizontal and vertical extent as well as internal branching patterns. Our findings revealed a significant relationship between the structural complexity (D_b) and the three measures of xylem safety along with K_s. Tree species with low structural complexity developed embolism-resistant xylem at the cost of hydraulic efficiency. Our findings also revealed that the D_b had a stronger and more significant relationship with branch hydraulic safety and efficiency compared to other structural attributes examined. We conclude that D_b seems to be a robust descriptor of tree architecture that relates to important branch hydraulic properties of a tree.

Keywords Drought tolerance · Fractal analysis · Hydraulic conductivity · Plant hydraulics · Tree architecture · Terrestrial laser scanning · Xylem safety

✉ Yonten Dorji
Yonten.dorji@uni-goettingen.de

1 Department for Spatial Structures and Digitization of Forests, Faculty of Forest Sciences, Georg-August-Universität Göttingen, Büsgenweg 1, 37077 Göttingen, Germany

2 Department of Forest Science, College of Natural Resources, Royal University of Bhutan, 1264 Punakha, Bhutan

3 Ecophysiology and Vegetation Ecology, Institute of Biological Sciences, University of Würzburg, Julius-Von-SachsJulius-Von-Sachs-Platz, 97082 Würzburg, Germany

4 Ecosystem Modeling Group, Center for Computational and Theoretical Biology, University of Würzburg, Klara-Oppenheimer-Weg 32, 97074 Würzburg, Germany

5 Biodiversity Modelling and Environmental Change, School of Biosciences, College of Life and Environmental Sciences, University of Birmingham, Birmingham B15 2TT, UK

6 Forest and Agroforest Systems, Technical University of Munich, Hans-Carl-V.-Carlowitz-Platz 2, 85354 Freising, Germany

7 Chair of Forest Botany, Institute of Forest Botany and Forest Zoology, Technical University of Dresden, Pienner Str. 7, 01737 Tharandt, Germany

Introduction

As a consequence of climate change, the occurrence of severe droughts is increasing in several parts of the world (Trenberth et al. 2014; Settele et al. 2015). While forest systems are susceptible to a variety of severe climatic conditions, drought and its concomitant disruptions have the largest impact worldwide (Reichstein et al. 2013). It is the most common stressor impacting the forest carbon balance, potentially generating a sharp decline in net primary productivity at regional and global levels (Ciais et al. 2005; Lewis et al. 2011). There has been increasing concern that warmer temperatures may cause more extended and intense droughts, highlighting the need for accurate projections of drought impacts on forest ecosystems (Rousi et al. 2022). In addition, studies revealed that drought-related mass tree death is not limited to drier locations (Anderegg et al. 2012; Hammond et al. 2022). It has been reported for a range of forest biomes, including cold temperate (Nardini et al. 2013; Schuldt et al. 2020) and tropical forests (Rowland et al. 2015). Evidence from studies by Nepstad et al. (2007) and Phillips et al. (2010) confirmed the significant impact of drought on the structural integrity and functional processes of trees. Drought-induced stress can lead to reduced growth rates, altered leaf physiology, compromised water transport efficiency, and increased susceptibility to secondary biotic factors. These combined negative impacts disrupt the overall structure and functioning of trees, potentially compromising their ability to thrive in arid environments.

Bittencourt et al. (2020) emphasized the critical role of the adaptability of trees in determining the trajectory of forest ecosystems in the face of climate change. With the increasing prevalence of dry climates, the ability of trees to adjust and withstand prolonged water scarcity will play a crucial role in how forests are structured and how resilient they are in the future (Seidel and Ammer 2023). Understanding and predicting the adaptive responses of trees to extended drought events is, therefore, crucial for effective forest management strategies and conservation efforts in the context of ongoing climate change. Therefore, it is of paramount importance to understand the relationship between tree architecture, forest structure, and drought tolerance.

The structure and function of a forest ecosystem are ultimately tied to the species composition and the structures of the individual trees (West et al. 2009; Seidel et al. 2019a). Various ecological functions and services offered by a forest, such as wood value (Ishii et al. 2004), recreational value (Ribe 2009), or ecosystem resilience (Neill and Puettmann 2013), depend on the structural characteristics and the species composition in the stand.

Tree structure and form are not the results of stochastic growth (Valladares and Niinemets 2007). They are, in fact, the result of the interaction between the genetic growth plan and the biotic and abiotic environment (Scorza et al. 2002; Busov et al. 2008). Environmental factors like wind (Watt et al. 2005), latitude (Kuuluvainen 1992), seed dispersal strategy (Dorji et al. 2021), water availability (Niinemets and Kull 1995), and competition (Dorji et al. 2019) determine the shape of a tree. The plasticity of tree geometry in response to environmental agents was considered to be the outcome of an individual's drive to maximize strength in a certain area (Borchert and Slade 1981), such as reproductive potential or sunlight absorption (Hollender and Dardick 2015).

There is a limited body of research pertaining to the correlation between tree structure and hydraulic properties. This underscores the significance of comprehending how structural traits influence a tree's ability to manage water stress, thereby contributing to a deeper understanding of plant adaptation mechanisms in challenging environmental conditions. For example, Huber values, representing sapwood-to-leaf area ratios, influence water transport efficiency (Apgaua et al. 2015; van der Sande et al. 2019). Leaf distribution across multiple branches optimizes water availability for photosynthesis (Niinemets 2007). Trees also exhibit traits like optimized branching angles, tapering, and wood density to balance safety and resource efficiency. (MacFarlane 2020). These relationships between tree structure and drought tolerance are complex. However, the insights mentioned above highlight the importance of structural traits in understanding drought tolerance and predicting forest responses to climate change. Further, numerous studies observed a higher drought sensitivity for 'larger' (higher crown surface area and crown volume, higher branch numbers and volume) trees in different biomes (e.g., Benett et al. 2015O'Brien et al. 2017; Stovall et al. 2019). It has been argued that their physiological susceptibility to drought in terms of water conductivity is the primary cause (Tyree and Zimmermann 2002; Fajardo and Piper 2021), leaving larger trees more susceptible to drought stress (McDowell and Allen 2015).

The study of 3D tree structure and form was shown to be of importance for a variety of disciplines, such as tree phylogenetics, remote sensing of forest landscapes, ecosystem modelling, and carbon stock computation (Chave et al. 2005; Arseniou and MacFarlane 2021; Arseniou et al. 2021). Despite this great importance, the three-dimensional quantification of tree architecture was a challenging task in the past (destructive, laborious, and time-consuming). So far, the assessment has been limited to only small trees (Moore and Maguire 2008; Bentley et al. 2013). Therefore, a lack of sufficient data has hampered the development and testing of

Table 1 Summary of all investigated tree species: the number of individual trees in each species, mean box-dimension (D_b), mean height (TTH), mean diameter at breast height (DBH), mean crown volume (CV), mean crown surface area (CSA), and total mean number of branches (1st, 2nd, and 3rd order branches)

Tree species	Total nos	Mean P_{12} (MPa)	Mean P_{50} (MPa)	Mean P_{88} (MPa)	Mean D_b	Mean TTH (m)	Mean DBH (cm)	Mean CV (m^3)	Mean CSA (m^2)	Mean no. of branches
Acer campestre	4	− 4.7211	− 5.4067	− 6.0923	1.831	7.00	10.53	13.33	36.60	31
Acer platanoides	4	− 3.5434	− 4.2756	− 5.0079	1.747	7.20	12.47	13.54	37.75	24
Acer rubrum	4	− 2.4991	− 2.8803	− 3.2616	1.892	6.18	8.86	12.98	36.23	33
Betula pendula	4	− 2.0034	− 2.3839	− 2.7645	1.893	8.42	11.18	19.31	54.74	37
Betula utilis	4	− 1.8456	− 2.0628	− 2.2800	1.882	6.56	9.01	13.39	36.30	24
Carpinus betulus	4	− 3.3497	− 4.6168	− 5.8840	1.927	7.45	10.78	9.63	30.39	33
Crataegus persimilis	4	− 4.6567	− 5.9116	− 7.1666	1.674	5.92	7.46	5.22	24.89	21
Ostrya carpinifolia	4	− 3.8300	− 4.5611	− 5.2923	1.874	6.02	8.97	11.51	34.06	26
Platanus acerifolia	4	− 1.5450	− 1.8528	− 2.1606	1.987	4.73	9.93	8.59	26.48	31
Platanus orientalis	4	− 1.2779	− 1.8010	− 2.3241	1.926	7.67	13.24	25.86	56.71	45
Prunus padus	3	− 2.2919	− 3.1274	− 3.9628	1.800	6.36	10.88	15.77	41.24	24
Prunus serrulata	4	− 2.8387	− 4.0144	− 5.1901	1.652	5.82	11.88	5.92	21.90	18
Pyrus calleryana	4	− 4.4818	− 5.7064	− 6.9311	1.870	7.56	10.84	9.37	32.62	25
Sorbus latifolia	4	− 3.8923	− 5.7420	− 7.5917	1.766	5.57	9.34	6.99	25.79	26
Tilia cordata	4	− 2.2878	− 3.1628	− 4.0379	1.909	6.50	11.51	11.34	33.46	28
Tilia mongolia	4	− 2.1461	− 2.9245	− 3.7029	1.803	5.10	8.75	2.38	15.87	27
Tilia platyphyllus	4	− 2.8096	− 3.3936	− 3.9776	1.946	7.57	12.25	14.51	38.91	30
Tilia tormentosa	4	− 2.6327	− 3.2876	− 3.9424	1.854	7.52	17.12	35.85	71.09	30

Measurement units are given within parentheses

The trees were grown at a minimum spacing of 3 × 3 m, as shown in Fig. 1. The study trees grew in the same soil, climate, and geographical positioning, i.e., the southwest-facing aspect with a gentle slope
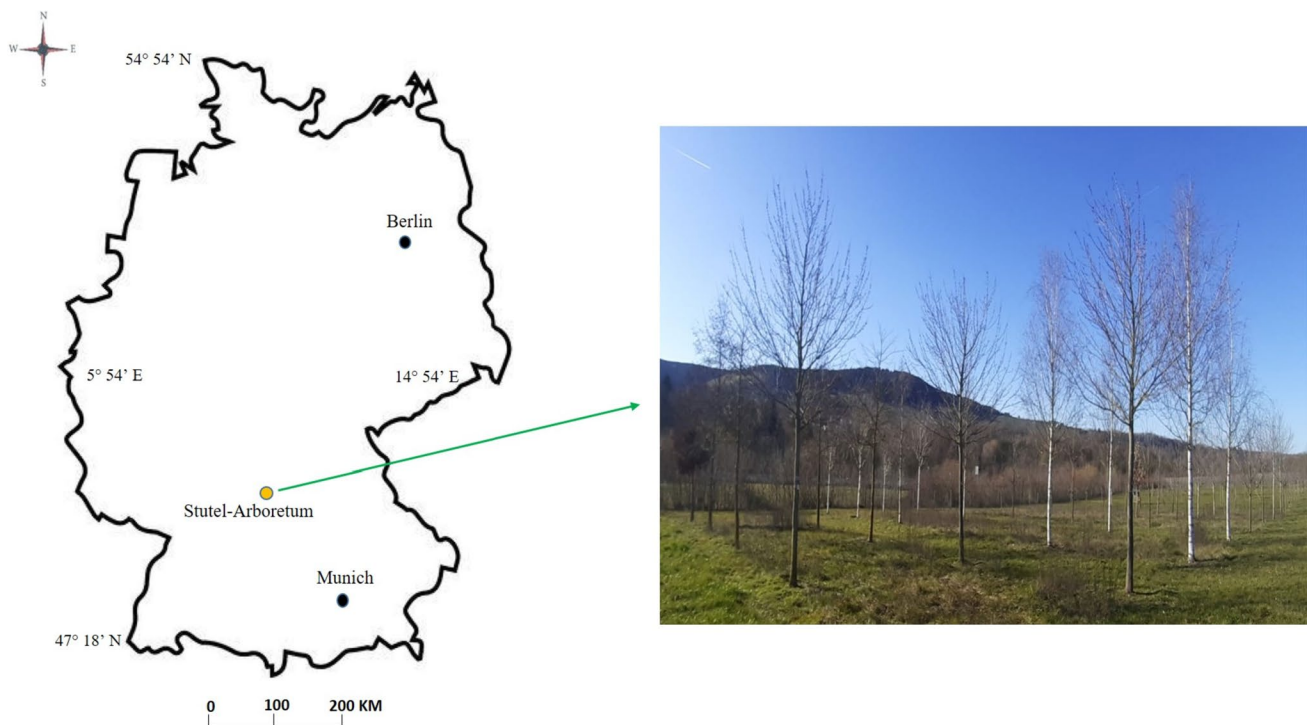
Fig. 1 Map and location of the research site at Stutel, Wuerzburg, Germany, and a photograph depicting a section of the Stutel-Arboretum

theory, specifically linking tree structures with their physiological role and mechanism (Malhi et al. 2018).

The arrival of laser scanning technology has transformed the way we perceive trees and quantify their structures (Gonzalez de Tanago et al. 2018). Besides conventional tree size attributes, TLS is also used to derive tree branching patterns (branch angles, lengths, volumes) with precision levels exceeding those of leading international allometric models (Liang et al. 2018; Demol et al. 2022). Thus, this has provided an avenue to analyze and understand how tree architecture and forest structure change in response to various factors, e.g., competition, drought, and forest management (e.g., Dassot et al. 2011; Heidenreich and Seidel 2022).

Our grasp of how plants adapt to dry spells and how drought-induced tree mortality occurs depends on understanding tree hydraulic traits (Choat et al. 2018). As one of the most commonly reported metrics of xylem vulnerability or hydraulic failure (Anderegg et al. 2016), hydraulic safety is often quantified by the water potential at which 12%, 50% and 88% loss of hydraulic conductivity occur (cf. Gleason et al. 2016). Embolisms form when water potentials in conduits drop to levels that promote embolism formation (Tyree and Zimmermann 2002). As a result, hydraulic thresholds related to xylem dysfunction are of major importance to understand the drought response of trees (Blackman et al. 2019; Britton et al. 2022; Hajek et al. 2022). Therefore, plant

hydraulic characteristics play an important role in drought survivability and carbon fluxes (Chen et al. 2021; McDowell et al. 2022).

To describe tree architecture, the box-dimension can be used (Seidel 2018). In simple words, it is calculated by dividing the tree into a series of boxes of different sizes and counting the number of boxes that the tree branches into depending on the size of these boxes (Seidel 2018). The higher the box-dimension, the more complex a tree is. The fractal-like geometry of trees, according to these concepts, is a direct representation of both intrinsic and malleable morphological features that influence tree development and survival (Hastings and Sugihara 1993; Halley et al. 2004).

We employed the box-dimension approach of fractal analysis in this study to quantify the overall tree architectural complexity. We assessed how this complexity relates to the hydraulic thresholds of xylem safety across a range of temperate diffuse-porous tree species. Specifically, we used detailed tree architectural measures related to branching patterns (up to the 3rd branching orders) to address the following research questions. We first tested whether (1) there exists a relationship between structural complexity and xylem safety or not? If a relationship exists, (2) we assume that the branch angles and lengths of the tree species have a significant relationship with xylem safety since the branching pattern relates to the hydraulic network. Since the tree structural complexity metric, the box-dimension (D_b), is a
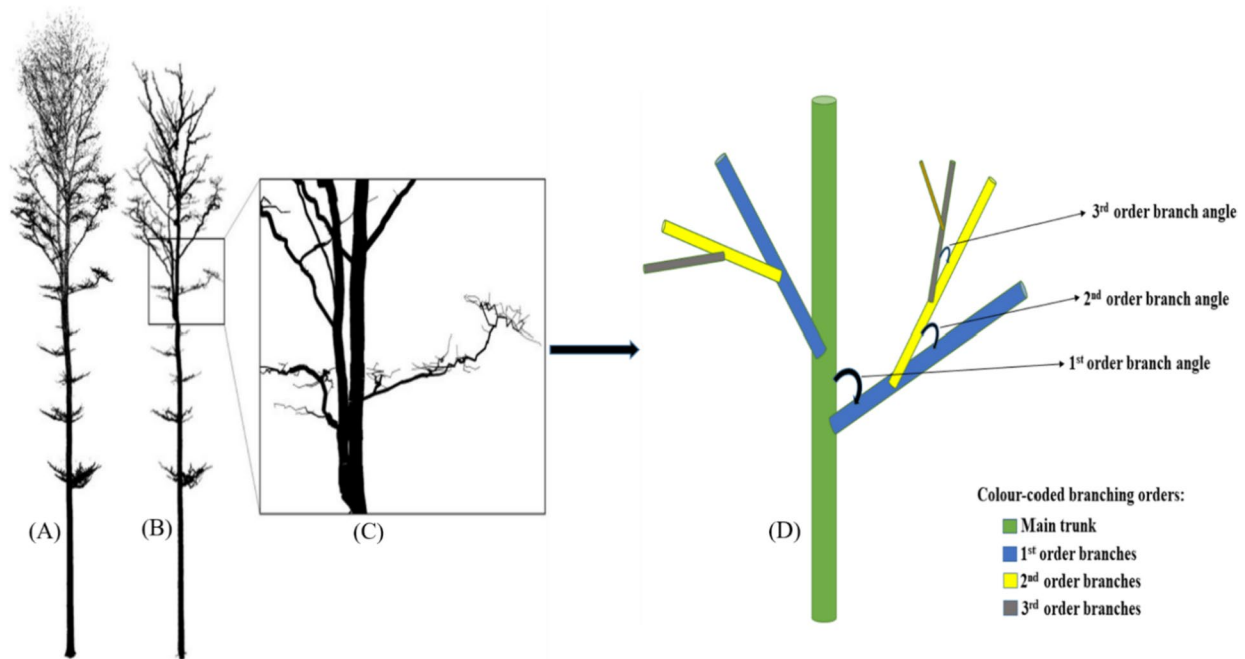
Fig. 2 Exemplary two-dimensional representation of a 3D point cloud of a tree in **A** and the corresponding Quantitative Structure Model in **B**. A close-up of QSM in **C** and a cylindrical demonstration of colour-coded branching patterns on the right end in **D**. Adapted and modified from Dorji et al. (2019) (Colour figure online)

holistic measure that incorporates overall tree architectural patterns, we finally speculate that (3) D_b will show a higher influence on the xylem safety compared to the other selected single tree structural characteristics.

Materials and methods

Study site

This research study is part of the extensive Klimabäume Stutel project managed under the Bavarian State Institute for Viticulture and Horticulture (LWG). The research was carried out at Stutel-Arboretum, located on the eastern bank of the river Main, near Wuerzburg, Bavaria, Germany, at an altitude of 180 m above sea level. The geographical coordinates are at 49°51′49″ N, 9°51′8″ E. The mean annual temperature of the area is 9.5 °C, receiving an average annual precipitation of 603 mm. A continental climate type characterizes the region, and the area, as such, experiences frequent drought events, especially in the hot summer months. Based on the data from German Meteorological Service (DWD) (2023) in Würzburg, Bavaria, Germany, frequent drought events occur from June to September, with a minimum monthly precipitation of 20 mm and

a maximum monthly mean temperature of 25°C. The soil is primarily sandy anthrosol with a pH value of 7.3. The arboretum is home to over 400 tree species. All trees were initially grown in various nurseries across Europe and Asia before being transplanted as seedlings (2 years of age) to the Stutel-Arboretum.

The plantations at the arboretum were established in 2010 by the LWG with the aim to examine the feasibility of trees of various species as future urban trees that are resilient to droughts. The trees in the arboretum are monitored for their growth development while experiencing the same climate conditions. However, they are kept in their natural state without disturbing their growth form and with no fertilization or irrigation applied.

Our research investigated 71 different tree individuals belonging to 18 species (see Table 1 for basic information on 18 species pooled together, and the data repository for detailed 71 individual tree information).

Terrestrial LiDAR

We used the Faro Focus M70 Terrestrial Laser Scanner (Faro Technologies Inc., Lake Mary, FL, USA) to obtain detailed three-dimensional point cloud data of all study trees. The instrument uses laser light with 905 nm wavelength for
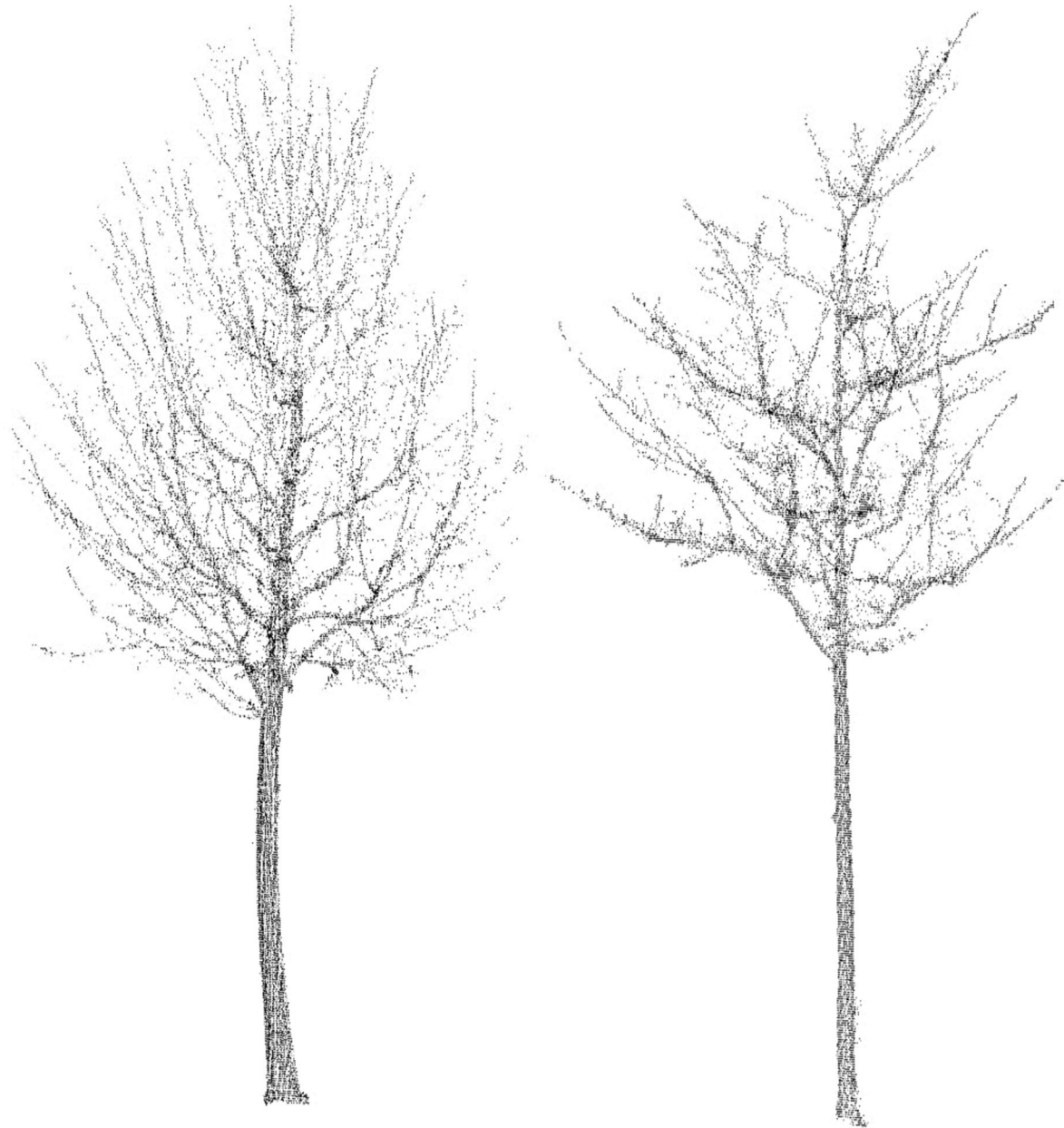
Fig. 3 Two exemplary three-dimensional tree point clouds with the highest (left) and lowest (right) box-dimension (D_b) values observed in our research study. On the left is a *Tilia cordata* tree ($D_b = 2.04$); on the right is an individual of *Crataegus persimilis* ($D_b = 1.55$)

scanning the environment up to a distance of 70 m and covers a field of view of $300° \times 360°$ with an angular resolution of 0.03 degrees, yielding 10,240 points per $360°$. The scanner was set up on a tripod at breast height (1.3 m) and levelled horizontally, employing a bubble level.

Scanning was carried out during a dry period with no wind (March 26, 2020) when the trees were in leafless condition (all study tree species were deciduous) to guarantee the best visibility of the entire wooden tree compartments. We performed a multi-scan procedure of all 71 trees, with four

scans each, amounting to a total of 284 scans. We scanned each tree from four corner points with the tree always in the center, also referred to as 'corner setup' in the literature (Zande et al. 2008). We applied the instrument's standard filters (clear contour and clear sky) during scanning. The scan data were then automatically registered, filtered, and exported as single xyz.-files using Faro Scene (Faro Technologies Inc., Lake Mary, FL, USA). The generated 3D image of each tree is a composite of millions of three-dimensional

measuring points, producing a precise and detailed replica of our study trees in the field.

Point cloud processing and quantitative structure models (QSM)

Each tree was manually segmented from the surrounding scenery in the scan using open-source CloudCompare software (CloudCompare v2.10.1, https://www.danielgm.net/cc/). CompuTree software (Vers. 5.0, CompuTree Group; http://computree.onf.fr/?page_id=42) was then used to generate QSMs (Quantitative Structure Models) for all 71 trees. A QSM model is a depiction of the tree point cloud constructed out of cylinders of diverse diameters and lengths. We applied the same QSM-parameter configurations for all trees to ensure the reproducibility of our observations. Clustering tolerance was set at 1 cm, with a maximum of 600-point clusters containing at least 400 points each. If less than 400 points were found per cluster, the software automatically adjusted the clustering size. Details can be found in

the documentation of CompuTree. For all 71 trees, we used QSM models to acquire detailed information on the branching architecture of the trees. We obtained the (1) total branch length, (2) mean branch angle up to 3rd order of branches, (3) mean branch length up to 3rd order of branches. An exemplary tree QSM with a cylindrical demonstration of branching patterns is depicted in Fig. 2.

The crown surface area of each tree was determined using the convex hull polygon approach introduced in Seidel et al. 2015. Using an algorithm written in Mathematica (Wolfram Research, Champaign, USA), we determined the surface of the convex hull polygons from the triangle points building the convex hull by applying Heron's formula (ref. Metz et al. (2013) for detail).

Similarly, for crown volume, we used a voxel-based method. In this approach, convex hulls are created around a horizontal slice through the tree crown that represents 10-cm thick layers, and the area of each "slice" is multiplied by 10 to calculate the volume of each slice. The total volume of all slices is then considered the tree crown volume.
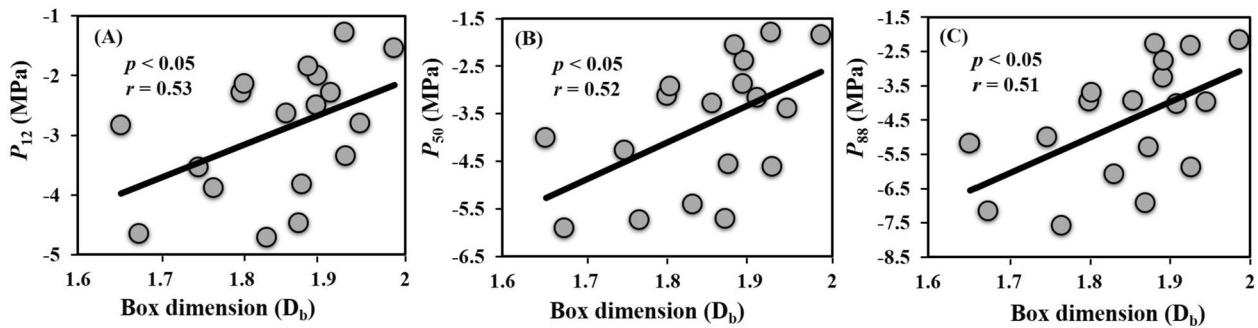

Fig. 4 Scatter plots showing the correlation between the mean structural complexity of the tree species represented by the box-dimension (D_b) and **A** = P_{12} (MPa), **B** P_{50} (MPa), and **C** P_{88} (MPa). The data were available and analyzed for $n = 18$ tree species (with a mean of 3–4 individuals per species). Regression lines are shown as solid black lines indicating significant relationships for all at $p < 0.05$, with Spearman's rank correlation ranging from $r = 0.51$–0.53
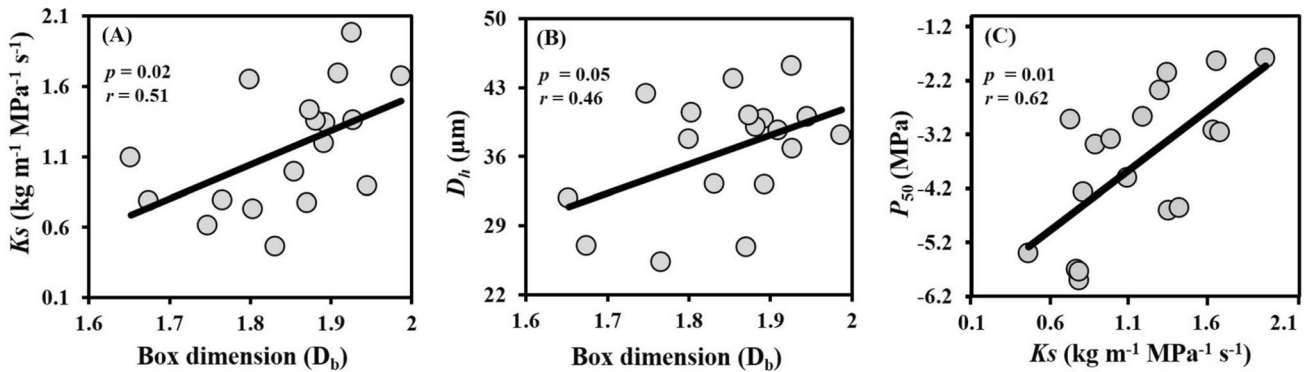
Fig. 5 Results of simple species-level linear regressions of box-dimension (D_b) in relation to **A** specific conductivity (K_s, kg m^{-1} MPa^{-1} s^{-1}) and **B** hydraulically weighted vessel diameter (D_h, μm). The **C** shows a significant correlation between P_{50} (MPa) and the specific conductivity (K_s, kg m^{-1} MPa^{-1} s.$^{-1}$)
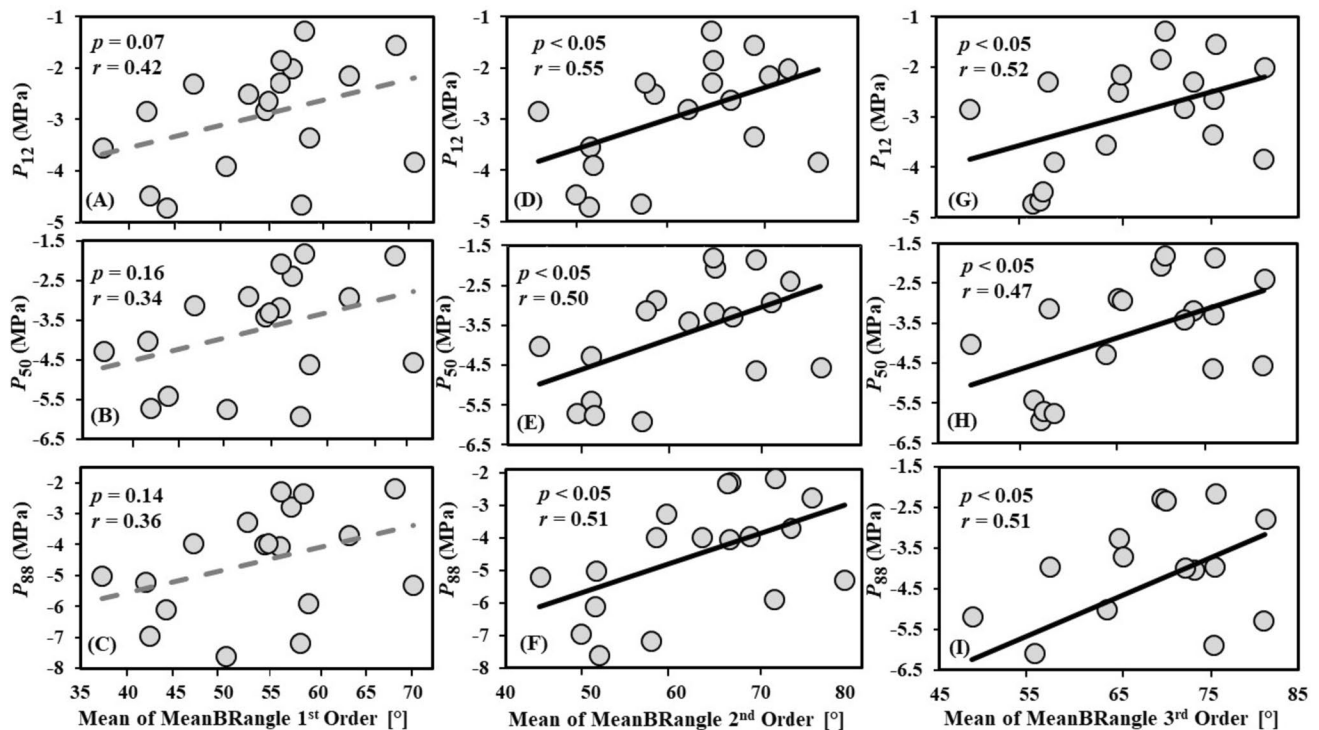
Fig. 6 Scatter plot for the three measures of xylem safety (P_{12}, P_{50}, P_{88}; MPa) over mean of mean branch angle (MeanBRangle [°]) of 1st order branches (**A**–**C**); MeanBRangle [°] of 2nd order branches (**D**–**F**) and 3rd order branches (**G**–**I**) of all species (shown as mean values). Black solid lines indicate significant relationships and dashed grey lines indicate non-significant relationships (**A**–**C**). Spearman's rank correlations ranged from $r = 0.34$–0.55; $n = 18$ species

Box-dimension (D_b)

The box-dimension (D_b) is a metric of structural complexity (Mandelbrot 1977). For a tree, it integrates all structural attributes, including crown dimensions and branching patterns (Seidel et al. 2019b). Box-dimension here was derived from single tree point clouds using the methods outlined by Seidel (Seidel 2018) and described in detail (including code) in Arseniou et al. (2021) (supplementary material: https://www.mdpi.com/article/https://doi.org/10.3390/rs13142773/s1). This technique is based on the concepts of Sarkar and Chaudhuri (Sarkar and Chaudhuri 1994) and Mandelbrot's breakthrough contribution (Mandelbrot 1977). In a nutshell, box-dimension was calculated by counting the number of boxes of a particular size required to encapsulate all aboveground tree structures in the 3D point cloud. The box-dimension is then determined as the slope of the regression line derived from a scatterplot of the number of boxes denoted by log (N) over the inverse of the logarithm of the respective box size, with the box size expressed in relation to the initial box size. The theoretical range of D_b of a single tree spans between 1 and 3 (Mandelbrot 1977). Figure 3 shows an exemplary point cloud of our study trees with the highest and lowest structural complexity, respectively.

Xylem embolism resistance

Leveraging the Cavitron instrument, vulnerability curves were measured using the flow-centrifuge technique (Cochard 2002; Cochard et al. 2005, 2013), constructed from a Sorval RC 5 series centrifuge with manual rotation speed control, and using Cavisoft software (Cavisoft v.5.2.1, University of Bordeaux, Bordeaux, France). Flow centrifuges increase water tension in xylem segments and measure the loss of hydraulic conductance simultaneously using a centrifugal force. The sample's susceptibility to cavitation is shown by the relationship between the percentage loss of xylem conductance (PLC) and xylem water tension. A subset of the vulnerability curve measurements discussed in this paper was used for addressing controversies in safety-vessel diameter relationships and for a methodological comparison with the pneumatic method (Paligi et al. 2021).

In total, 71 branches of at least 60 cm in length (for data on vessel length distribution, refer to Paligi et al. 2023) from the Stutel arboretum (mean diameter at basipetal end $\pm$ SE: 8.87 ± 0.10 mm; $n = 71$) were sampled from the middle of the canopy at the height of c. 4–5 m from June to September in 2019 and 2020, wrapped in wet paper towels, bagged in the dark, humidified plastic bags, transported to the laboratory and processed on the same day. In the laboratory,
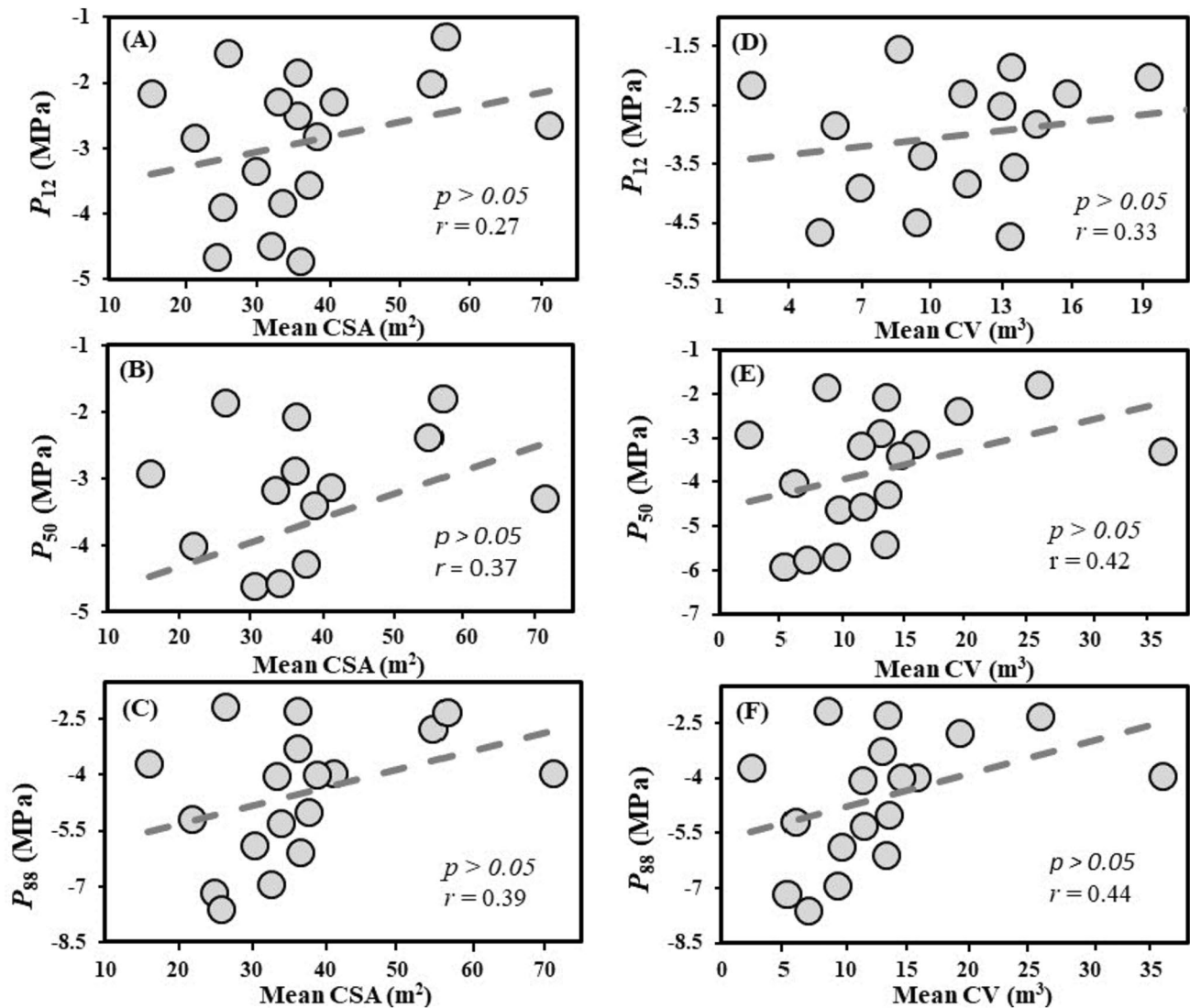
Fig. 7 Scatter plots of the three measures of xylem safety (**A** P_{12}, **B** P_{50}, **C** P_{88}; MPa) against the crown surface area (CSA, [m.^{2}]) of all the studied trees (mean per species). Similarly, the scatterplots **D–F** show a correlation between different mean xylem safety, P_{12}, P_{50}, and P_{88}, with the Crown Volume (CV), respectively. Regression lines are shown as dashed lines, indicating non-significant. The data were available and analyzed for $n = 18$ species. Spearman's rank correlations ranged from $r = 0.27$ to 0.44

samples were submerged in water and recut several times using pruning shears to a final length of 27.5 cm to release the tension in the xylem (Torres-Ruiz et al. 2015). Lateral leaves and twigs were removed, and lateral branches were evened with a razor blade to fit the sample into the Cavitron.

Before measurement in the Cavitron, the bark of the branch samples was removed at both sample ends for 4 cm. Both basipetal and acropetal end diameters were measured two times before insertion into the rotor with cuvettes on both sample ends. Vulnerability curves were measured in the Cavitron without prior flushing at high pressure and using ultrapure deionized and degassed water containing 10 mM KCl and 1 mM CaCl$_2$ (Delzon et al. 2010; Schuldt et al. 2016). Conductance measurement started at a water

potential of -0.834 MPa (equivalent to 3000 rotations per minute, rpm). Then, by raising the rotating speed and the conductivity (K) gauged at each pressure level, the xylem pressure was gradually lowered.

Measurements were ended after the samples lost at least 90% of their initial conductance, which was recorded with Cavisoft software (Table 1). A 2-min waiting time was maintained before measuring at each pressure step to ensure stable conductance values.

Vulnerability curves were then fitted in R (v. 4.1.0, R Core Team 2023) with nonlinear least squares using the logistic model by Pammenter and Van der Willigen (1998) in a modified version based on raw conductivity measurements (Ogle et al. 2009):
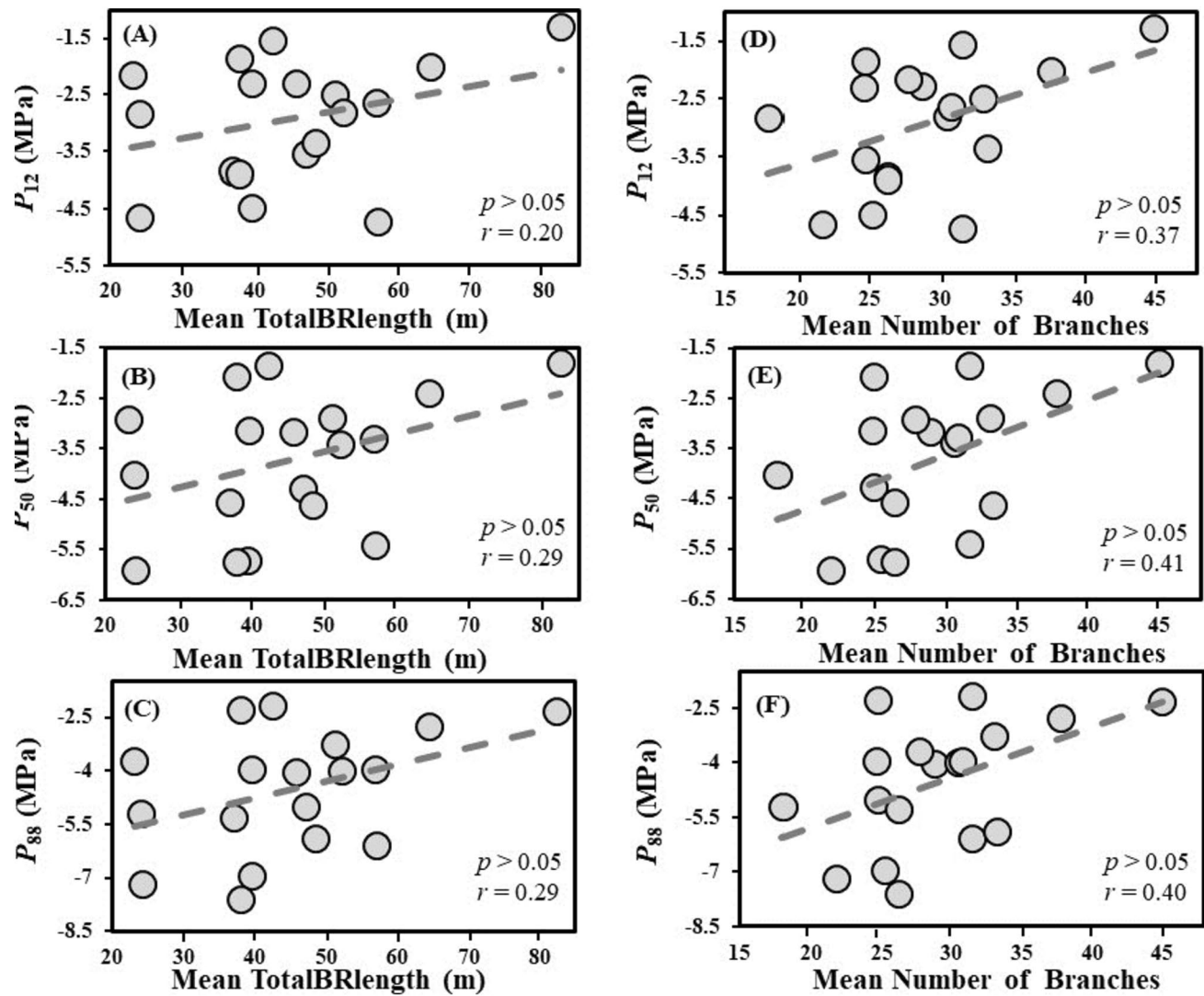
Fig. 8 Scatter plots of the three measures of xylem safety (**A** P_{12}, **B** P_{50}, **C** P_{88}; MPa) against total branch length (TotalBRlength [m]). Similarly, the scatterplots **D**–**F** show the relationship between xylem safety measures (P_{12}, P_{50}, P_{88}) over the mean number of branches of all tree species, respectively. All the above data were available and analyzed for $n=18$ species of 71 tree individuals. Regression lines are shown as dashed grey lines to indicate non-significant relationships

$$k_i \sim \mathrm{Normal}\left(k_{\mathrm{sat}} \cdot \left(1 - \frac{1}{1 + \exp\left(-\frac{s_{50}}{25}(P_i - P_{50})\right)}\right), \sigma\right) \quad (1)$$

where for each observation i, the conductivity k_i is assumed to be normally distributed around a logistic function of the water potential P_i with the parameters P_{50} (water potential at 50% loss of conductivity), S_{50} (corresponding slope of the vulnerability curve on the percent loss of conductivity scale), ksat (initial conductivity at full saturation) and residual standard deviation σ. The calculation was repeated for P_{12} and P_{88}.

Wood anatomy and hydraulic efficiency

Semi-thin transverse sections for wood anatomical analyses were cut from the same branch samples used for hydraulic measurements with a sliding microtome (G.S.L.1, Schenkung Dapples, Zürich, Switzerland), stained with safranin-alcian blue, rinsed with distilled water and ethanol (95%), and permanently mounted on glass slides using Euparal (Carl Roth, Karlsruhe, Germany). A light microscope equipped with an automated table and a digital camera (Observer. Z1, Carl Zeiss MicroImaging GmbH, Jena, Germany; Software: AxioVision c4.8.2, Carl Zeiss MicroImaging GmbH) was used for digitizing the complete cross-section at 100-times magnification. Image processing was done with GIMP

v2.10.6 (GIMP Development Team 2018, https://www.gimp.org/) and the particle analysis function from ImageJ v1.52p (Schneider et al. 2012). We calculated vessel diameters (D, μm) from minor (a) and major vessel radii (b) as

$$D = ((32 \times (a \times b)^3)/(a^2 + b^2))^{1/4}, \tag{2}$$

according to White (1991) and used D to calculate the hydraulically weighted average vessel diameter (D_h, μm) according to Sperry et al. (1994) as

$$D_h = \Sigma D^5 / \Sigma D^4. \tag{3}$$

For measuring branch sapwood area-specific hydraulic conductivity (K_s, kg m s^{-1} MPa^{-1}) with degassed, demineralized water containing 10 mM KCl and 1 mM CaCl$_2$ using a Xylem Plus embolism meter (Bronkhorst, Montigny-Les-Cormeilles, France), fresh samples were rehydrated in water for 20 min and recut to 35 cm length underwater. To prevent leakage, lateral twigs were removed and the cuts were immediately sealed with a quick-drying adhesive (Loctite 431 with activator 7452; Henkel, Düsseldorf, Germany). After measuring initial hydraulic conductivity at a low-pressure head of 6 kPa for 5 min, samples were repeatedly flushed at high pressure of 120 kPa for 10 min to remove potential emboli to measure maximum hydraulic conductivity (K_h, kg m^{-1} MPa^{-1} s^{-1}) once the conductivity values were stable. K_s was calculated by dividing K_h by the basipetal cross-sectional area excluding the bark.

Statistical analysis

All statistical analyses were performed in software R (v. 4.1.0, R Core Team 2023). We used linear regression to analyze the correlation between the xylem safety (represented by pressures inducing 12%, 50%, and 88% losses of stem hydraulic conductance) and different tree architectural attributes. To begin, we looked at the relationship between the overall tree structural complexity (D_b) and the xylem safety at P_{12}, P_{50}, P_{88}. We also performed species-level linear regression of the box-dimension (D_b) in relation to the specific conductivity (K_s) and the hydraulically weighted vessel diameter (D_h) of the corresponding tree species. Furthermore, we tested the relationship between all the tree architectural attributes like CSA (Crown Surface Area), CV (Crown Volume), branch angles, branch lengths, branch numbers, and branch volume with the xylem safety measures (P_{12}, P_{50}, P_{88}) using correlation analysis (Spearman's rank). To test whether the assumption of independence of linear regression was violated by possible phylogenetic signal in the residuals, we calculated Pagel's λ (Pagel 1999), a measure of phylogenetic signal, of the residuals of each model, and used the likelihood ratio tests to assess whether λ was significantly different from 0 (meaning no phylogenetic signal), with the phylosig() function from the phytools R package (v. 2.0.3, Revell 2012). In the case of

significant phylogenetic signal in the residuals, we calculated additional Phylogenetic Least Squares (PGLS) regressions using the ape (v. 5.7.1, Paradis and Schliep 2019) and nlme (v. 3.1.162, Pinheiro et al. 2023) packages (Revell 2010; Symonds and Blomberg 2014). More details on the method are provided in the "Appendix".

The significance level was kept at $p < 0.05$ for all the above tests, and data were averaged per species. This was done to identify whether the relationships between the structural variables and hydraulic risk are detectable despite differences in wood anatomy between species.

Results

Overall, we observed a large range in structural complexity for the investigated trees, given that all individuals were growing under identical conditions. The values ranged from 1.55 to 2.04 units of D_b (see Fig. 3 for visualization), with a mean value of 1.85 and a standard deviation of 0.11 units of D_b. Within single species, box-dimension showed some natural variation, as one would expect, ranging from only

Table 2 Results from the likelihood ratio tests that assess whether Pagel's λ of the residual errors is different from 0

Response	Predictor	λ	Log-likelihood (λ)	Likelihood ratio ($\lambda = 0$)	p value
P_{12}	D_b	> 0.01	− 23.98	− 8.29	1.000
P_{50}	D_b	0.71	− 27.39	0.51	0.473
P_{88}	D_b	0.75	− 30.98	0.84	0.359
K_s	D_b	0.33	− 6.41	0.66	0.418
D_h	D_b	0.26	− 53.88	0.85	0.357
P_{50}	**K_s**	**0.71**	**− 23.38**	**3.97**	**0.046**
P_{12}	BrA1	0.76	− 23.93	1.72	0.189
P_{50}	**BrA1**	**0.89**	**− 26.41**	**5.49**	**0.019**
P_{88}	**BrA1**	**0.92**	**− 29.51**	**7.57**	**0.006**
P_{12}	BrA2	0.81	− 22.69	2.03	0.154
P_{50}	**BrA2**	**0.93**	**− 24.55**	**6.25**	**0.012**
P_{88}	**BrA2**	**0.96**	**− 27.42**	**8.48**	**0.004**
P_{12}	BrA3	0.86	− 22.82	2.48	0.115
P_{50}	**BrA3**	**0.98**	**− 24.50**	**6.67**	**0.010**
P_{88}	**BrA3**	**1.01**	**− 27.20**	**8.92**	**0.003**
P_{12}	CSA	0.59	− 24.41	1.92	0.166
P_{50}	CSA	0.66	− 28.02	2.72	0.099
P_{88}	CSA	0.66	− 31.80	2.89	0.089
P_{12}	CV	0.50	− 24.51	1.25	0.263
P_{50}	CV	0.58	− 28.20	1.90	0.168
P_{88}	CV	0.59	− 31.99	2.12	0.146

Cases where a significant difference was found are highlighted in bold font

Apart from the abbreviation used in the main text: BrA1-3: Mean of BRangle 1st–3rd order; CSA: MeanCSA, CV: MeanCV

0.05 units of D_b within *Platanus Acerifolia* and up to 0.25 units for *Crataegus persimilis*.

The box-dimension for all trees, pooled by species, showed a significant positive correlation with the three measures of xylem safety, i.e., the water potentials at 12%, 50% and 88% loss of hydraulic conductance (P_{12}, P_{50}, P_{88}) (Fig. 4). The strongest correlation was found with the P_{12} value and the lowest with P_{88}, although all three correlation coefficients were very close ($r = 0.51$ to $r = 0.53$; Fig. 4).

We further observed a close relationship between specific hydraulic conductivity (K_s, kg m^{-1} MPa^{-1} s^{-1}) of the branches and D_b (Fig. 5A), while the hydraulically weighted vessel diameter was only related to D_b at marginal significance (Fig. 5B).

Furthermore, the relationships between mean branch angles and xylem safety (P_{12}, P_{50}, P_{88}) showed a positive trend for all branch orders. Despite quite some scatter, the relationship was statistically significant for 2nd and 3rd order branches but not for the first order branches (see Fig. 6).

The xylem safety showed no significant relationship with the CSA (crown surface area) nor the CV (crown volume) (Fig. 7).

The same pattern was observed for xylem safety (P_{12}, P_{50} and P_{88}) over the mean total branch length (Fig. 8D, E, F) and mean total number of branches (Fig. 8D, E, F), with positive trends but no significant relationships.

For 7 of the 21 tested relationships, significant phylogenetic signal was found in the residuals of the linear regression, namely the relationship between K_s and P_{50}, and all relationships of P_{50} and P_{88} with branch angles of the 1st–3rd order. While a PGLS of P_{50} in dependency of K_s still yielded a significant positive slope, the relationships between xylem safety measures and branch angles were not significant in PGLS regressions (see "Appendix"). For the box-dimension-xylem safety relationship, no phylogentic signal was found.

Discussion

Trees comprise a complex branching network that needs to be able to support the foliar tissue with water, even in the most distal twigs. The water conducting xylem plays a crucial role in maintaining efficient hydraulic conductivity within this system. The breakdown of this water transport system due to acute water deficit has been identified as a primary factor causing drought-induced tree mortality (Arend et al. 2021; Nolan et al. 2021; Hajek et al. 2022).

We set out to further our understanding of the relationship between tree architecture and the drought tolerance of trees. To begin with, we tested whether the trees' overall structural complexity would be related to xylem safety. Our findings reveal that the tree's structural complexity,

represented by box-dimension (D_b), is related to its xylem safety. The results showed that the increase in D_b increases the hydraulic vulnerability to embolism formation when exposed to water stress. We found that the box-dimension (D_b) as a holistic measure of tree architectural complexity showed a significant correlation with the three measures of xylem safety of the respective tree species, i.e., the water potentials at 12%, 50% and 88% loss of hydraulic conductivity. In fact, the strongest observed relationship in our entire data was between D_b and xylem safety (compare *r* values of Fig. 4 to all subsequent figures). It was stronger than that of other laser-based measures related to the sheer tree crown dimension (Fig. 7). The laser-based measures describing the branching geometry (branching angles) also showed significant relationships with xylem safety, with correlation values up to 0.55 (Fig. 6, although the results were not stable after correcting for phylogenetic non-independence, see "Appendix"), thus partly supporting our second research claim, where we hypothesized the significant relationship between the branching geometry and the xylem safety. However, no significant relationship was observed for branch length. Finally, the third hypothesis and research claim were confirmed, as the xylem safety measures were more closely related to the holistic measure of tree structural complexity (D_b) than to the other single selected measures of tree architecture (comp. Fig. 5 to subsequent figures).

Our data indicate that the higher the branch angles and the more complex the architectural complexity of a tree species (i.e., higher D_b values), the lower is the xylem safety (ability to resist embolism formation).

The impact of tree complexity on drought stress becomes evident when comparing trees with different D_b values. A tree with higher D_b would experience elevated drought stress compared to a tree with lower D_b. This is because a tree with higher D_b possesses a more intricate crown, which accommodates a larger crown network area. As a result, the tree's greater photosynthetic area in the more complex crown leads to increased drought vulnerability during times of drought stress (due to a higher hydraulic resistance within the system).

While species-specific functional traits certainly result in different responses to drought stress because of varying vessel systems and branch sizes across the species (Olson and Rosell 2013; Hajek et al. 2014; Arseniou and MacFarlane 2021), our findings indicate that across various species, the complexity of the hydraulic architecture and the greater photosynthetic area associated with a greater D_b (e.g., Seidel et al. 2019b) relates to an increased risk of vulnerability to embolism. A higher total leaf area consequently results in a greater demand for water (Arseniou and MacFarlane 2021),

which is also mirrored by the observed relationship between branch hydraulic efficiency and the complexity of the crown. Across the similar-aged temperate trees of our sample, species with a more complex crown had branches with a higher specific hydraulic conductivity (K_s) to support a greater total leaf area (cf. Seidel et al. 2019b) at the cost of xylem safety. The D_b integrates all architectural patterns, like the branch angles, branch numbers, branch length, crown surface area, crown volume, DBH, height, and many other tree architectural attributes, and translates them into a single physiologically meaningful number (Seidel et al. 2019b). Conventional measures of tree size quantify this insufficiently. Our data indicate that future studies should focus on the complexity of the hydraulic system. The conductive path length and the complexity of the hydraulic system, described not only by the box-dimension but also by the branching angles, were shown to be related to xylem safety. We argue that a reduced gravitational resistance exists when branches are more horizontal (flatter and lower angles). This helps explain why branching geometry plays a significant role not only in light interception but also in carbon and water fluxes between trees and the atmosphere (Iwasa et al. 1985; Enquist et al. 2009; Forrester et al. 2018; Dorji et al. 2021). Hence and as indicated earlier, these complex tree architectural attributes, in particular D_b, in regular times contribute to higher vigour and strength of the trees (e.g., Seidel et al. 2019b). However, in times of severe droughts, they become a liability, as they result in greater water demand to sustain the ecophysiological processes. Overall, tree species with high structural complexity (high D_b values) developed in our sample an efficient but vulnerable xylem compared to species with lower structural complexity (low D_b values), which developed embolism-resistant xylem at the cost of hydraulic efficiency. In this sense, future research could investigate whether species occurring in more water-stressed environments are then selected to evolve simpler architectural attributes.

It is important to stress that our data were obtained from trees growing in isolation without competition for light or space. In closed forests, microclimate and shading might alter the effects observed here. However, some of the observed patterns might equally apply to forest trees, for example, the observed relationship between the branch angles and hydraulic vulnerability.

Finally, tree species (or provenances of the same species) of lower D_b might be favored for plantation in drought-prone regions (or provenances) rather than species with higher D_b because the latter might be vulnerable to more stress and disturbance when exposed to drought.

Conclusion

Our findings shed new light on the relationship between tree architecture and hydraulic vulnerability. The combined use of TLS and fractal analysis provided a holistic measure of architectural complexity (D_b). The D_b was shown to relate most strongly to the hydraulic vulnerability of our study trees. The branch xylem of tree species with a more complex crown, which most likely supports a higher total leaf area, appeared to be most vulnerable to drought-induced hydraulic failure. More difficult-to-access laser-based measures of detailed branching angles are also related significantly to the hydraulic failure risk of the trees. However, these measures were also outperformed by the holistic measure, the D_b.

From our data, we can conclude that structurally complex trees are more vulnerable to drought-induced hydraulic failure than trees of simpler structures when growing in the open. It is important to note that our study trees were all growing without competition, in full exposure to the sun. In closed forest stands, microclimatic effects, soil moisture, and other stand-level parameters might be decisive and potentially result in a different picture. Our study is one of the first to clearly and empirically highlight the relationship between the architectural complexity of the hydraulic system and the hydraulic vulnerability of trees.

Appendix

Testing for phylogenetic signal in residual errors of linear regressions

One of the main assumptions of linear regression is the independence of errors (Gelman et al. 2021, p. 154). This assumption is commonly hurt in multi-species analyses by the phenomenon that more closely related species tend to have more similar traits (Symonds & Blomberg 2014, p. 105). To test whether phylogenetic non-independence of errors is an issue in our regressions, we tested whether there is a significant phylogenetic signal in the residuals of all regression analyses conducted in this study. In the case of significant phylogenetic signal, a Phylogenetic Generalized Least Square (PGLS) regression would be necessary, whereas otherwise, a standard linear regression is appropriate (Revell 2010).

We used the R package V.PhyloMaker (v. 0.1.0, Jin and Qian 2019) to prune an underlying megatree ('BGOTB. extended.tre') to the species in this study to obtain their phylogeny. As a measure of phylogenetic signal, we calculated

Fig. 9 Two examples illustrating the distribution of residual errors throughout the phylogeny. The relationship of P_{50} in dependency of box-dimension is the main relationship of interest in this study and had no significant evidence for a phylogenetic signal different from 0 in the residuals. The relationship of P_{88} in dependency of Mean branch angle of the 3rd order was among the regression analyses in this study the one with the highest estimate for Pagel's λ in the residuals (Colour figure online)
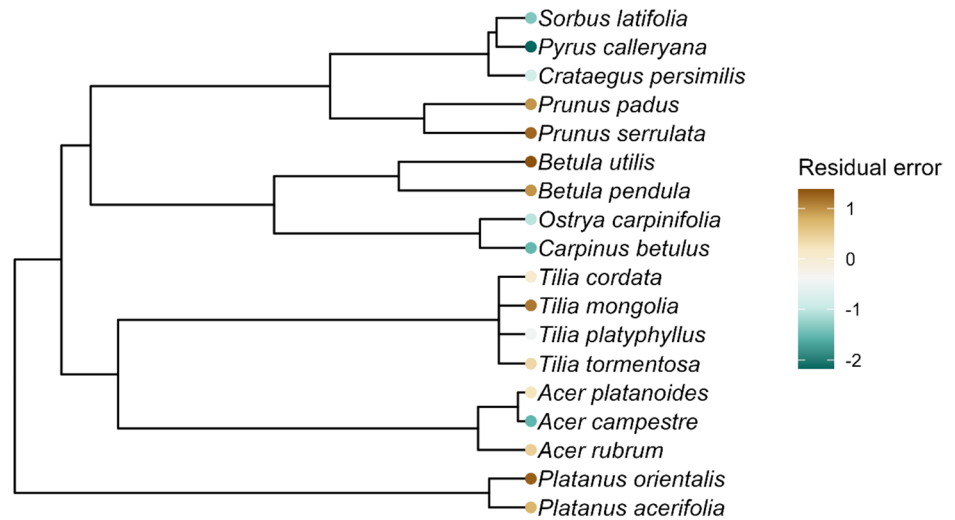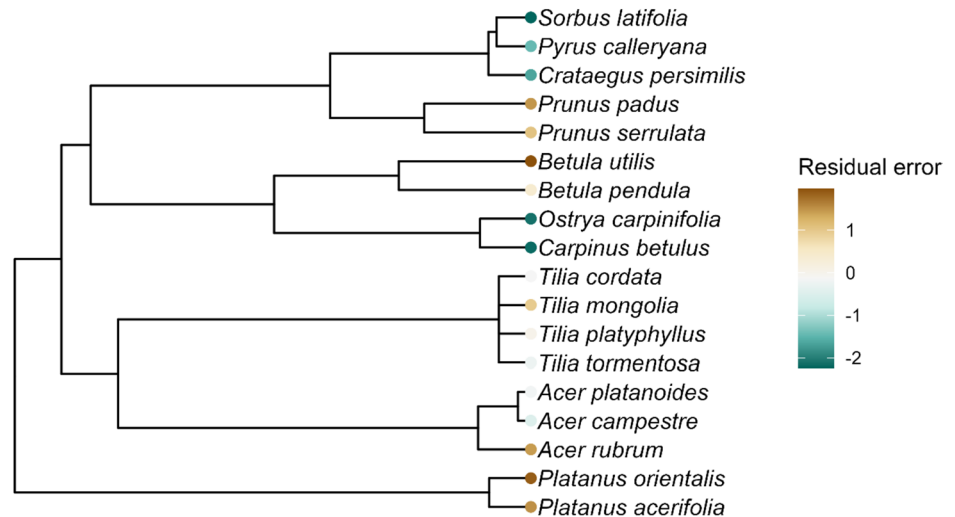
Pagel's λ (Pagel 1999) with the phylosig () function from the phytools R package (v. 2.0.3, Revell 2012). Simultaneously, the function also performs a likelihood ratio test for the null hypothesis of $\lambda = 0$, meaning no phylogenetic signal. Therefore, in case of non-significant test results, there is no evidence for a phylogenetic signal different from 0 (Table 2; Fig. 9).

The results show that phylogenetic non-independence was not an issue in most tested relationships. Especially the relationships with box-dimension, the main predictor of interest in this study, were not affected. For the cases where significant phylogenetic signal was found, we conducted additional PGLS analyses and present the results here. We first used the function corPagel () from the R package ape (v. 5.7.1, Paradis & Schliep 2019) to create a phylogenetic variance–covariance matrix based on the species' phylogeny, and then fitted a PGLS model with the nlme package (v. 3.1.162, Pinheiro et al. 2023), using the phylogenetic variance–covariance matrix as correlation structure (Fig. 10).
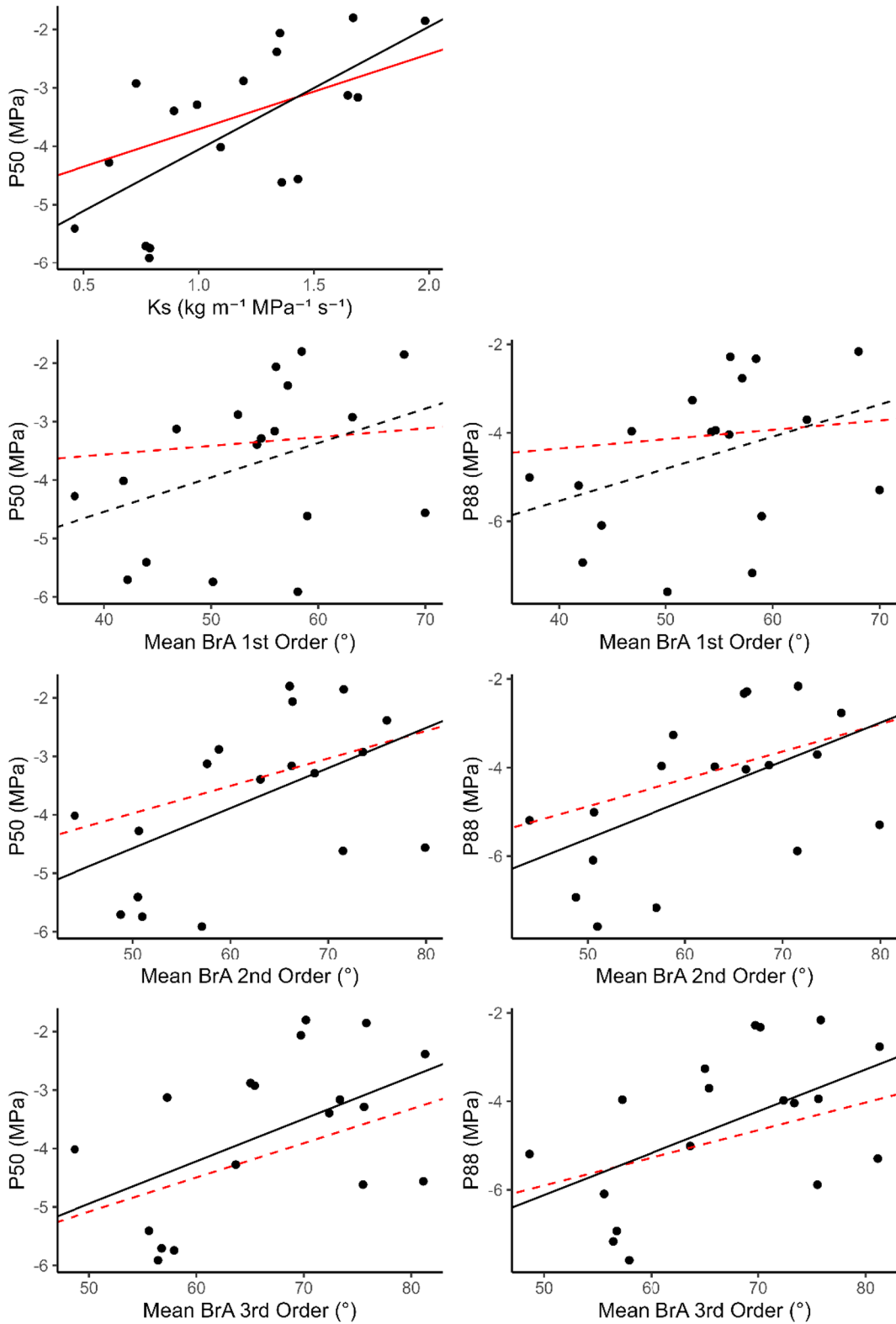
Fig. 10 Regression lines from PGLS analyses (red) compared with linear regressions (black) for all pairwise relationships with significant phylogenetic signals in their residuals. Solid lines indicate slope parameters significantly different from 0 ($p < 0.05$), and dashed lines indicate non-significant slope parameters (Colour figure online)

Declarations

Conflict of interest The authors declare no conflict of interest.

Code availability The code will be made available upon request (please contact the corresponding author).

References

Anderegg WR, Berry JA, Smith DD, Sperry JS, Anderegg LD, Field CB (2012) The roles of hydraulic and carbon stress in a widespread climate-induced forest die-off. Proc Natl Acad Sci 109:233–237. https://doi.org/10.1073/pnas.1107891109

Anderegg WR, Klein T, Bartlett M, Sack L, Pellegrini AF, Choat B, Jansen S (2016) Meta-analysis reveals that hydraulic traits explain cross-species patterns of drought-induced tree mortality across the globe. Proc Natl Acad Sci 113(18):5024–5029. https://doi.org/10.1073/pnas.1525678113

Apgaua DMG, Ishida FY, Tng DYP, Laidlaw MJ, Santos RM, Rumman R, Eamus D, Holtum JAM, Laurance SGW (2015) Functional traits and water transport strategies in lowland tropical rainforest trees. PLoS ONE 10(6):e0130799. https://doi.org/10.1371/journal.pone.013079910.1073/pnas.1525678113

Arend M, Link RM, Patthey R, Hoch G, Schuldt B, Kahmen A (2021) Rapid hydraulic collapse as cause of drought-induced

mortality in conifers. Proc Natl Acad Sci 118:e2025251118. https://doi.org/10.1073/pnas.2025251118

Arseniou G, MacFarlane DW (2021) Fractal dimension of tree crowns explains species functional-trait responses to urban environments at different scales. Ecol Appl 31(4):e02297. https://doi.org/10.1073/pnas.2025251118

Arseniou G, MacFarlane DW, Seidel D (2021) Measuring the contribution of leaves to the structural complexity of urban tree crowns with terrestrial laser scanning. Remote Sens 13:2773. https://doi.org/10.3390/rs13142773

Bentley LP, Stegen JC, Savage VM, Smith DD, von Allmen EI, Sperry JS, Reich PB, Enquist BJ (2013) An empirical assessment of tree branching networks and implications for plant allometric scaling models. Ecol Lett 16:1069–1078. https://doi.org/10.1111/ele.12127

Bittencourt PR, Oliveira RS, da Costa AC, Giles AL, Coughlin I, Costa PB, Bartholomew DC, Ferreira LV, Vasconcelos SS, Barros FV, Junior JA (2020) Amazonia trees have limited capacity to acclimate plant hydraulic properties in response to long-term drought. Global Change Biol 26(6):3569–3584. https://doi.org/10.1111/gcb.15040

Borchert R, Slade NA (1981) Bifurcation ratios and the adaptive geometry of trees. Bot Gaz 142(3):394–401. https://doi.org/10.1086/337238

Britton TG, Brodribb TJ, Richards SA, Ridley C, Hovenden MJ (2022) Canopy damage during a natural drought depends on species identity, physiology and stand composition. New Phytol 233(5):2058–2070. https://doi.org/10.1111/nph.17888

Busov VB, Brunner AM, Strauss SH (2008) Genes for control of plant stature and form. New Phytol 77(3):589–607. https://doi.org/10.1111/j.1469-8137.2007.02324.x

Chave J, Andalo C, Brown S, Cairns MA, Chambers JQ, Eamus D, Fölster H, Fromard F, Higuchi N, Kira T, Lescure JP (2005) Tree allometry and improved estimation of carbon stocks and balance in tropical forests. Oecologia 45(1):87–99. https://doi.org/10.1007/s00442-005-0100-x

Chen S, Tang D, Tao S, Liu P, Mathews JP (2021) Implications of the in-situ stress distribution for coalbed methane zonation and hydraulic fracturing in multiple seams, western Guizhou. China J Petrol Sci Eng 204:108755. https://doi.org/10.1016/j.petrol.2021.108755

Choat B, Brodribb TJ, Brodersen CR, Duursma RA, López R, Medlyn BE (2018) Triggers of tree mortality under drought. Nature 558:531–539. https://doi.org/10.1038/s41586-018-0240-x

Ciais P, Reichstein M, Viovy N, Granier A, Ogée J, Allard V, Aubinet M, Buchmann N, Bernhofer C, Carrara A, Chevallier F (2005) Europe-wide reduction in primary productivity caused by the heat and drought in 2003. Nature 437(7058):529–533. https://doi.org/10.1038/nature03972

Cochard H (2002) A technique for measuring xylem hydraulic conductance under high negative pressures. Plant Cell Environ 25:815–819. https://doi.org/10.1046/j.1365-3040.2002.00863.x

Cochard H, Damour G, Bodet C, Tharwat I, Poirier M, Améglio T (2005) Evaluation of a new centrifuge technique for rapid generation of xylem vulnerability curves. Physiol Plantarum 124:410–418. https://doi.org/10.1111/j.1399-3054.2005.00526.x

Cochard H, Badel E, Herbette S, Delzon S, Choat B, Jansen S (2013) Methods for measuring plant vulnerability to cavitation: a critical review. J Exp Bot 64:4779–4791. https://doi.org/10.1093/jxb/ert193

Dassot M, Constant T, Fournier M (2011) The use of terrestrial LiDAR technology in forest science: application fields, benefits and challenges. Ann for Sci 68:959–974. https://doi.org/10.1007/s13595-011-0102-2

Delzon S, Douthe C, Sala A, Cochard H (2010) Mechanism of water-stress induced cavitation in conifers: bordered pit structure and

function support the hypothesis of seal capillary-seeding. Plant Cell Environ 33(12):2101–2111. https://doi.org/10.1111/j.1365-3040.2010.02208.x

Dorji Y, Annighöfer P, Ammer C, Seidel D (2019) Response of beech (*Fagus sylvatica* L.) trees to competition—new insights from using fractal analysis. Remote Sens 11(22):2656. https://doi.org/10.3390/rs11222656

Dorji Y, Schuldt B, Neudam L, Dorji R, Middleby K, Isasa E, Körber K, Ammer C, Annighöfer P, Seidel D (2021) Three-dimensional quantification of tree architecture from mobile laser scanning and geometry analysis. Trees 35(4):1385–1398. https://doi.org/10.1007/s00468-021-02124-9

Enquist JB, West BG, Brown HJ (2009) Extensions and evaluations of a general quantitative theory of forest structure and dynamics. Proc Natl Acad Sci USA 106(17):7040–7051

Fajardo A, Piper FI (2021) How to cope with drought and not die trying: drought acclimation across tree species with contrasting niche breadth. Funct Ecol 35(9):1903–1913. https://doi.org/10.1111/1365-2435.13861

Forrester DI, Ammer C, Annighöfer PJ, Barbeito I, Bielak K, Bravo-Oviedo A, Coll L, del Río M, Drössler L, Heym M, Hurt V (2018) Effects of crown architecture and stand structure on light absorption in mixed and monospecific *Fagus sylvatica* and *Pinus sylvestris* forests along a productivity and climate gradient through Europe. J Ecol 106(2):746–760. https://doi.org/10.1111/1365-2745.12803

Gelman A, Hill J, Vetahri A (2021) Regression and other stories. Cambridge University Press, Cambridge, UK

German Meteorological Service (DWD). (2023). Würzburg—climate data. Retrieved from https://dwd.de/EN/climate_environment/climate_monitoring/normals/deutschland/index.html.

Gleason SM, Westoby M, Jansen S, Choat B, Hacke UG, Pratt RB, Bhaskar R, Brodribb TJ, Bucci SJ, Cao KF, Cochard H, Delzon S, Domec JC, Fan Z, Feild TS, Jacobsen AL, Johnson DM, Lens F, Maherali H, Martínez-Vilalta J, Mayr S, McCulloh KA, Mencuccini M, Mitchell PJ, Morris H, Nardini A, Pittermann J, Plavcová L, Schreiber SG, Sperry JS, Wright IJ, Zanne AE (2016) Weak tradeoff between xylem safety and xylem-specific hydraulic efficiency across the world's woody plant species. New Phytol 209(1):123–136. https://doi.org/10.1111/nph.13646

Gonzalez de Tanago J, Lau A, Bartholomeus H, Herold M, Avitabile V, Raumonen P, Martius C, Goodman RC, Disney M, Manuri S, Burt A (2018) Estimation of above-ground biomass of large tropical trees with terrestrial LiDAR. Methods Ecol Evol 9(2):223–234. https://doi.org/10.1111/2041-210X.12904

Hajek P, Leuschner C, Hertel D, Delzon S, Schuldt B (2014) Tradeoffs between xylem hydraulic properties, wood anatomy and yield in *Populus*. Tree Physiol 34(7):744–756. https://doi.org/10.1093/treephys/tpu048

Hajek P, Link RM, Nock CA, Bauhus J, Gebauer T, Gessler A, Kovach K, Messier C, Paquette A, Saurer M, Scherer-Lorenzen M (2022) Mutually inclusive mechanisms of drought-induced tree mortality. Global Change Biol 28:3365–3378. https://doi.org/10.1111/gcb.16146

Halley JM, Hartley S, Kallimanis AS, Kunin WE, Lennon JJ, Sgardelis SP (2004) Uses and abuses of fractal methodology in ecology. Ecol Lett 7(3):254–271. https://doi.org/10.1111/j.1461-0248.2004.00568.x

Hammond WM, Williams AP, Abatzoglou JT, Adams HD, Klein T, López R, Sáenz-Romero C, Hartmann H, Breshears DD, Allen CD (2022) Global field observations of tree die-off reveal hotter-drought fingerprint for Earth's forests. Nat Commun 13:1761. https://doi.org/10.1038/s41467-022-29289-2

Hastings HM, Sugihara G (1993) Fractals: a user's guide for the natural sciences. Oxford Science Publications, Oxford

Heidenreich MG, Seidel D (2022) Assessing forest vitality and forest structure using 3D data: a case study from the Hainich National Park, Germany. Frontiers in Forests and Global Change 5:929106. https://doi.org/10.3389/ffgc.2022.929106

Hollender CA, Dardick C (2015) Molecular basis of angiosperm tree architecture. New Phytol 206(2):541–556. https://doi.org/10.1111/nph.13204

Ishii HT, Tanabe SI, Hiura T (2004) Exploring the relationships among canopy structure, stand productivity, and biodiversity of temperate forest ecosystems. For Sci 50:342–355. https://doi.org/10.1093/forestscience/50.3.342

Iwasa YO, Cohen DA, Leon JA (1985) Tree height and crown shape, as results of competitive games. J Theor Biol 112(2):279–297. https://doi.org/10.1016/S0022-5193(85)80288-5

Jin Y, Qian H (2019) V.PhyloMaker: an R package that can generate very large phylogenies for vascular plants. Ecography 42(8):1353–1359. https://doi.org/10.1111/ecog.04434

Kuuluvainen T (1992) Tree architectures adapted to efficient light utilization: is there a basis for latitudinal gradients? Oikos 65:275–284. https://doi.org/10.2307/3545019

Lewis SL, Brando PM, Phillips OL, van der Heijden GMF, Nepstad D (2011) The 2010 Amazon drought. Science 331:554. https://doi.org/10.1126/science.1200807

Liang X, Hyyppä J, Kaartinen H, Lehtomäki M, Pyörälä J, Pfeifer N, Holopainen M, Brolly G, Francesco P, Hackenberg J, Huang H (2018) International benchmarking of terrestrial laser scanning approaches for forest inventories. ISPRS J Photogramm 144:137–179. https://doi.org/10.1016/j.isprsjprs.2018.06.021

MacFarlane DW (2020) Functional relationships between branch and stem wood density for temperate tree species in North America. Front for Glob Change 3:63. https://doi.org/10.3389/ffgc.2020.00063

Malhi Y, Jackson T, Patrick Bentley L, Lau A, Shenkin A, Herold M, Calders K, Bartholomeus H, Disney MI (2018) New perspectives on the ecology of tree structure and tree communities through terrestrial laser scanning. Interface Focus 8(2):20170052. https://doi.org/10.1098/rsfs.2017.0052

Mandelbrot BB (1977) The fractal geometry of nature. W.H. Freeman Company, New York

McDowell NG, Allen CD (2015) Darcy's law predicts widespread forest mortality under climate warming. Nat Clim Change 5:669–672. https://doi.org/10.1038/nclimate2641

McDowell NG, Sapes G, Pivovaroff A, Adams HD, Allen CD, Anderegg WR, Arend M, Breshears DD, Brodribb T, Choat B, Cochard H (2022) Mechanisms of woody-plant mortality under rising drought, CO_2 and vapour pressure deficit. Nat Rev Earth Environ 3(5):294–308. https://doi.org/10.1038/s43017-022-00272-1

Moore JR, Maguire DA (2008) Simulating the dynamic behavior of Douglas-fir trees under applied loads by the finite element method. Tree Physiol 28:75–83. https://doi.org/10.1093/treephys/28.1.75

Nardini A, Battistuzzo M, Savi T (2013) Shoot desiccation and hydraulic failure in temperate woody angiosperms during an extreme summer drought. New Phytol 200:322–329. https://doi.org/10.1111/nph.12288

Neill AR, Puettmann KJ (2013) Managing for adaptive capacity: Thinning improves food availability for wildlife and insect pollinators under climate change conditions. Can J for Res 43:428–440. https://doi.org/10.1139/cjfr-2012-0345

Nepstad DC, Tohver IM, Ray D, Moutinho P, Cardinot G (2007) Mortality of large trees and lianas following experimental drought in an Amazon Forest. Ecology 88:2259–2269. https://doi.org/10.1890/06-1046.1

Niinemets U (2007) Photosynthesis and resource distribution through plant canopies. Plant Cell Environ 30(9):1052–1071. https://doi.org/10.1111/j.1365-3040.2007.01683.x

Niinemets Ü, Kull O (1995) Effects of light availability and tree size on the architecture of assimilative surface in the canopy of Picea abies: variation in needle morphology. Tree Physiol 15(5):307–315. https://doi.org/10.1093/treephys/15.5.307

Nolan RH, Gauthey A, Losso A, Medlyn BE, Smith R, Chhajed SS, Fuller K, Song M, Li X, Beaumont LJ, Boer MM (2021) Hydraulic failure and tree size linked with canopy dieback in eucalyptus forest during extreme drought. New Phytol 230:1354–1365. https://doi.org/10.1111/nph.17298

O'Brien MJ, Engelbrecht BM, Joswig J, Pereyra G, Schuldt B, Jansen S, Kattge J, Landhäusser SM, Levick SR, Preisler Y, Väänänen P, Macinnis-Ng C (2017) A synthesis of tree functional traits related to drought-induced mortality in forests across climatic zones. J Appl Ecol 54(6):1669–1686

Ogle K, Barber JJ, Willson C, Thompson B (2009) Hierarchical statistical modeling of xylem vulnerability to cavitation. New Phytol 182:541–554. https://doi.org/10.1111/j.1469-8137.2008.02760.x

Olson ME, Rosell JA (2013) Vessel diameter–stem diameter scaling across woody angiosperms and the ecological causes of xylem vessel diameter variation. New Phytol 197(4):1204–1213. https://doi.org/10.1111/nph.12097

Pagel M (1999) Inferring the historical patterns of biological evolution. Nature 401:877–884. https://doi.org/10.1038/44766

Paligi S, Link RM, Isasa E, Bittencourt P, Cabral JS, Jansen S, Oliveira R, Pereira L, Schuldt B (2023) Assessing the agreement between the pneumatic and the flow-centrifuge method for estimating xylem safety in temperate diffuse-porous tree species. Plant Biol 25:1171–1185

Paligi S, Link RM, Isasa E, Bittencourt P, Cabral JS, Jansen S, Oliveira RS, Pereira L, Schuldt B (2021) Accuracy of the pneumatic method for estimating xylem vulnerability to embolism in temperate diffuse-porous tree species. bioRxiv. https://doi.org/10.1101/2021.02.15.431295

Pammenter NV, Van der Willigen C (1998) A mathematical and statistical analysis of the curves illustrating vulnerability of xylem to cavitation. Tree Physiol 18:589–593. https://doi.org/10.1093/treephys/18.8-9.589

Paradis E, Schliep K (2019) ape 5.0: an environment for modern phylogenetics and evolutionary analyses in R. Bioinformatics 35:526–528. https://doi.org/10.1093/bioinformatics/bty633

Phillips OL, Van Der Heijden G, Lewis SL, López-González G, Aragão LE, Lloyd J, Malhi Y, Monteagudo A, Almeida S, Dávila EA, Amaral I (2010) Drought–mortality relationships for tropical forests. New Phytol 187(3):631–646. https://doi.org/10.1111/j.1469-8137.2010.03359.x

Pinheiro J, Bates D, R Core Team (2023) nlme: linear and nonlinear mixed effects models. R package version 3.1-162. https://CRAN.R-project.org/package=nlme.

Reichstein M, Bahn M, Ciais P, Frank D, Mahecha MD, Seneviratne SI, Zscheischler J, Beer C, Buchmann N, Frank DC, Papale D (2013) Climate extremes and the carbon cycle. Nature 500(7462):287–295. https://doi.org/10.1038/nature12350

Revell LJ (2010) Phylogenetic signal and linear regression on species data. Methods Ecol Evol 1:319–329. https://doi.org/10.1111/j.2041-210X.2010.00044.x

Revell LJ (2012) phytools: An R package for phylogenetic comparative biology (and other things). Methods Ecol Evol 3:217–223. https://doi.org/10.1111/j.2041-210X.2011.00169.x

Ribe RG (2009) In-stand scenic beauty of variable retention harvests and mature forests in the US Pacific Northwest: The effects of basal area, density, retention pattern and down wood. J Environ Manage 91:245–260. https://doi.org/10.1016/j.jenvman.2009.08.014

Rousi E, Kornhuber K, Beobide-Arsuaga G (2022) Accelerated western European heatwave trends linked to more-persistent double

jets over Eurasia. Nat Commun 13:3851. https://doi.org/10.1038/s41467-022-31432-y

Rowland L, da Costa AC, Galbraith DR, Oliveira RS, Binks OJ, Oliveira AA, Pullen AM, Doughty CE, Metcalfe DB, Vasconcelos SS, Ferreira LV (2015) Death from drought in tropical forests is triggered by hydraulics not carbon starvation. Nature 528:119–122. https://doi.org/10.1038/nature15539

Sarkar N, Chaudhuri BB (1994) An efficient differential box-counting approach to compute fractal dimension of image. IEEE T Syst Man Cyb 24:115–120. https://doi.org/10.1109/21.259692

Schneider CA, Rasband WS, Eliceiri KW (2012) NIH Image to ImageJ: 25 years of image analysis. Nat Methods 9:671–675. https://doi.org/10.1038/nmeth.2089

Schuldt B, Knutzen F, Delzon S, Jansen S, Müller-Haubold H, Burlett R, Clough Y, Leuschner C (2016) How adaptable is the hydraulic system of European beech in the face of climate change-related precipitation reduction? New Phytol 210(2):443–458. https://doi.org/10.1111/nph.13798

Schuldt B, Buras A, Arend M, Vitasse Y, Beierkuhnlein C, Damm A, Gharun M, Grams TE, Hauck M, Hajek P, Hartmann H (2020) A first assessment of the impact of the extreme 2018 summer drought on Central European forests. Basic Appl Ecol 45:86–103. https://doi.org/10.1016/j.baae.2020.04.003

Scorza R, Bassi D, Liverani A (2002) Genetic interactions of pillar (columnar), compact, and dwarf peach tree genotypes. J Am Soc Hortic Sci 127(2):254–261. https://doi.org/10.21273/JASHS.127.2.254

Seidel D (2018) A holistic approach to determine tree structural complexity based on laser scanning data and fractal analysis. Ecol Evol 8:128–134. https://doi.org/10.1002/ece3.3661

Seidel D, Ammer C (2023) Towards a causal understanding of the relationship between structural complexity, productivity, and adaptability of forests based on principles of thermodynamics. For Ecol Manage 544:121238. https://doi.org/10.1016/j.foreco.2023.121238

Seidel D, Schall P, Gille M, Ammer C (2015) Relationship between tree growth and physical dimensions of *Fagus sylvatica* crowns assessed from terrestrial laser scanning. iForest 8(6):735. https://doi.org/10.3832/ifor1566-008

Seidel D, Ehbrecht M, Dorji Y, Jambay J, Ammer C, Annighöfer PJ (2019a) Identifying architectural characteristics that determine tree structural complexity. Trees 33:911–919. https://doi.org/10.1007/s00468-019-01827-4

Seidel D, Annighöfer P, Stiers M, Zemp CD, Burkardt K, Ehbrecht M, Ammer C (2019b) How a measure of tree structural complexity relates to architectural benefit-to-cost ratio, light availability, and growth of trees. Ecol Evol 9(12):7134–7142. https://doi.org/10.1002/ece3.5281

Settele J, Scholes R, Betts RA, Bunn S, Leadley P, Nepstad D, Overpeck JT, Taboada MA, Fischlin A, Moreno JM, Root T (2015) Terrestrial and inland water systems. In: Climate change 2014 impacts, adaptation and vulnerability: part A: global and sectoral. Cambridge University Press, Cambridge, pp 271–360. https://doi.org/10.1017/CBO9781107415379.009

Skelton RP, West AG, Dawson TE (2015) Predicting plant vulnerability to drought in biodiverse regions using functional traits. Proc Natl Acad Sci 112:5744–5749. https://doi.org/10.1073/pnas.1503376112

Sperry JS, Nichols KL, Sullivan JEM, Eastlack SE (1994) Xylem embolism in ring-porous, diffuse-porous, and coniferous trees of Northern Utah and Interior Alaska. Ecology 75:1736–1752. https://doi.org/10.2307/1939633

Stovall AE, Shugart H, Yang X (2019) Tree height explains mortality risk during an intense drought. Nat Commun 10(1):1–6. https://doi.org/10.1038/s41467-019-12380-6

Symonds MRE, Blomberg SP (2014) A primer on phylogenetic generalized least squares. In: Garamszegi LZ (ed) Modern phylogenetic comparative methods and their application in evolutionary biology. Springer, Berlin

Torres-Ruiz JM, Jansen S, Choat B, McElrone AJ, Cochard H, Brodribb TJ, Badel E, Burlett R, Bouche PS, Brodersen CR, Li S (2015) Direct X-ray microtomography observation confirms the induction of embolism upon xylem cutting under tension. Plant Physiol 167:40–43. https://doi.org/10.1104/pp.114.249706

Trenberth KE, Dai A, Van Der Schrier G, Jones PD, Barichivich J, Briffa KR, Sheffield J (2014) Global warming and changes in drought. Nat Clim Change 4(1):17–22. https://doi.org/10.1038/nclimate2067

Tyree MT, Zimmermann MH (2002) Hydraulic architecture of whole plants and plant performance. Xylem structure and the ascent of sap. Springer, Berlin, pp 175–214

van der Sande MT, Poorter L, Schnitzer SA, Engelbrecht BM, Markesteijn L (2019) The hydraulic efficiency–safety trade-off differs between lianas and trees. Ecology 100(5):e02666. https://doi.org/10.1002/ecy.2666

Watt MS, Moore JR, McKinlay B (2005) The influence of wind on branch characteristics of Pinus radiata. Trees 19(1):58–65. https://doi.org/10.1007/s00468-004-0363-6

West GB, Enquist BJ, Brown JH (2009) A general quantitative theory of forest structure and dynamics. Proc Natl Academy of Sciences 106:7040–7045. https://doi.org/10.1073/pnas.0812294106

White FM (1991) Viscous fluid flow. McGraw-Hill, New York

Zande DVD, Jonckheere I, Stuckens J, Verstraeten WW, Coppin P (2008) Sampling design of ground-based lidar measurements of forest canopy structure and its effect on shadowing. Can J Remote Sens 34:526–538. https://doi.org/10.5589/m08-070